ELSEVIER

Environmental Modelling & Software 15 (2000) 87–100

Environmental Modelling & Software

www.elsevier.com/locate/envsoft

# Relationships between topographically expressed zones of flow accumulation and sites of fault intersection: analysis by means of digital terrain modelling

Igor V. Florinsky [a,b,*]

[a] *Institute of Mathematical Problems of Biology, Russian Academy of Sciences, Pushchino, Moscow Region, 142292, Russia*
[b] *Land Resource Unit, Brandon Research Centre, Agriculture and Agri-Food Canada, Room 360, Ellis Building, University of Manitoba, Winnipeg, Manitoba, R3T 2N2, Canada*

Received 23 July 1998; accepted 27 July 1999

**Abstract**

Topographically expressed zones of flow accumulation often coincide with fault intersections because of increased rock fracturing. We have conducted a study of the interrelationships between topographically expressed accumulation zones and fault intersections, and the function of these sites in landscape evolution. The investigation has been performed with the use of digital terrain models, geological and soil data for the Crimean Peninsula. First, we carried out an analysis of associations of sites of fault intersections, intensive rock fracturing and abnormally high discharges of springs and boreholes, relating to fault intersections, with three types of landform element (zones of flow accumulation, transit and dissipation). We found that all phenomena under study are closely associated with topographically expressed accumulation zones. This has demonstrated that, within these zones, the soil moisture is influenced both by upward transport of deep-seated groundwater and by accumulation of overland lateral flows. Second, we predicted the effect of topography on irrigation-induced changes in the salt regime of soils and the groundwater level, assuming that topographically expressed accumulation zones can be marked by properties of fault intersections. We found that water leaking out of the North Crimean Canal can result in secondary salinisation of soils and a considerable rise of the watertable within some accumulation zones located downslope. Salts collected in the accumulation zones, and their slow movement through rock fractures, can lead to salinisation of the aquifers. We believe that topographically expressed accumulation zones are areas of contact and substance exchange between overland lateral and deep flows. 

*Keywords:* Digital terrain model; Topography; Fault; Fracture zone; Overland flow; Accumulation; Salinisation; Watertable

**Software availability**

Name of software: LANDLORD
Developer: I.V. Florinsky, T.I. Grokhlina, N.L. Mikhailova, G.L. Andrienko, N.V. Andrienko and P.V. Kozlov, Institute of Mathematical Problems of Biology, Russian Academy of Sciences, Pushchino, Moscow Region, 142292, Russia. Fax: +7-967-73-24-08; email: flor@impb.serpukhov.su, florinskyi@em.agr.ca
Year first available: 1994
Hardware required: PC 486dx, 16 MB RAM
Software required: MS Windows 3.xx, 95
Program language: C++
Program size: 976 kB
Availability and cost: Available at a cost of US$2000

## 1. Introduction

Relief generally affects substance movement; that is, migration and accumulation of water, mineral and organic substances over the landsurface and in the soil by gravity (Young, 1972; Gerrard, 1981). In turn, relief depends partly on geological structure (Meshcheryakov, 1965; Ollier, 1981). For example, valleys determine principal routes of surface flow. Valley networks are

* Tel.: +1-204-474-6120; fax: +1-204-474-7633.
*E-mail address:* florinskyi@em.agr.ca (I.V. Florinsky)

1364-8152/00/$ - see front matter 
PII: S1364-8152(99)00025-0

often connected with faults (Gerasimov and Korzhuev, 1979; Ollier, 1981) which can serve as pathways for upward transport of deep-seated substances to the landsurface (e.g., Kerrich, 1986). Therefore, some portions of surface flow routes can coincide with some discharges of deep-seated substance pathways. The study of these associations can be useful to gain a better understanding of the relationships between: (1) geological structures and landforms, and (2) endogenic and exogenic processes influencing landscape evolution.

Gravity-driven overland and intrasoil transport can be interpreted in terms of divergence or convergence and deceleration or acceleration of flow (Shary, 1995). Deceleration or acceleration of flow is determined by vertical (or profile) landsurface curvature ($k_v$). $k_v$ is the curvature of a normal section of the landsurface; this section includes the gravity acceleration vector at a given point on the landsurface. Flow tends to accelerate when $k_v>0$, and to decelerate when $k_v<0$ (Speight, 1974; Shary, 1991). Divergence or convergence of flow is controlled by horizontal (or plan) landsurface curvature ($k_h$). $k_h$ is the curvature of a normal section of the landsurface; this section is perpendicular to the section with $k_v$. Flow diverges when $k_h>0$, and converges when $k_h<0$ (Kirkby and Chorley, 1967; Shary, 1991). Notice that $k_h$ and $k_v$, among other topographic attributes, are of frequent use in landscape investigations carried out with digital terrain models (Moore et al., 1991; Shary et al., 1991; Florinsky, 1998).

Flow convergence and deceleration result in the accumulation of substances at soils caused by slowing down or termination of overland and intrasoil transport. On different scales, the intensity of these processes and the spatial distribution of accumulated substances can depend on the spatial distribution of the following landform elements (Shary et al., 1991).

- Elements characterised both by convergence and by deceleration of flow; that is, by both $k_h<0$ and $k_v<0$ [topographically expressed zones of flow accumulation, or *accumulation zones* (Fig. 1)]. Other authors have described these elements as areas of concave plan and profile shapes (Yefremov, 1949), areas of concave radial and contour lines (Troeh, 1964), concave–concave forms (Krcho, 1983) and convergent-footslope areas (Pennock et al., 1987).
- Elements offering both divergence and acceleration of flow; that is, both $k_h>0$ and $k_v>0$ [topographically expressed zones of flow dissipation, or *dissipation zones* (Fig. 1)]. Other authors have described these elements as areas of convex plan and profile shapes (Yefremov, 1949), areas of convex radial and contour lines (Troeh, 1964), convex–convex forms (Krcho, 1983) and divergent-shoulder areas (Pennock et al., 1987).
- Elements that are free of a concurrent action of flow convergence and deceleration as well as flow divergence and acceleration; that is, values of $k_h$ and $k_v$ have different signs or are zero [topographically expressed zones of flow transit, or *transit zones* (Fig. 1)].

Micro-depressions (plan sizes range from several decimetres to several meters) — that is, accumulation zones at the micro-topographic scale — control the spatial distribution of the wettest parts of the soil cover and hence determine soil and plant properties (Rode, 1953; Fedoseev, 1959). In arid and semiarid regions build-up of salts and groundwater salinisation occur in meso-depressions (plan sizes range from several tens to several hundreds of meters) and macro-depressions (plan sizes reach several kilometres and more), whereas micro-depressions are not salt-affected because they are washed out with rainfall at regular intervals (Kovda, 1971). Shallow groundwaters (Ivanova, 1960), landslides (Lanyon and Hall, 1983), soil gleying, maximum thickness of humus and carbonate horizons (Pennock et al., 1987), rock fracturing, increased hydraulic conductivity, increased aquifer discharges (Lukin, 1987), source areas of overland flows (Wood et al., 1990), saturation zones (Feranec et al., 1991) and increased pollution (Gurov and Kertsman, 1991) were found in topographically expressed accumulation zones in humid regions.

Fault intersections are important features of the Earth's crust (Poletaev, 1992). Looseness, fracturing and permeability of rocks (Poletaev, 1992), increased seismicity (Gelfand et al., 1972), landslide formation (Karakhanyan, 1981), active erosion and karst development (Korobeynik et al., 1982), swamp development (Trifonov et al., 1983) and abnormally high discharges of springs and boreholes (Morozov et al., 1988) occur at fault intersections. These sites can control intensive magmatism, volcanism (Poletaev, 1992), ore fields and deposits (Kutina, 1969; Fyodorov et al., 1989), and oil and gas fields (Dolenko et al., 1967).

Trifonov et al. (1983) were probably the first to establish an association of some relief depressions with fault intersections using remotely sensed data. Poletaev (1992) found *qualitatively* that, as a rule, fault intersections are topographically expressed by depressions. Florinsky (1993) proved *quantitatively* that topographically expressed accumulation zones can coincide with fault intersections. Indeed, mapping of $k_h$ and $k_v$ reveals two groups of topographically expressed lineaments (Florinsky, 1992). Structures of the first group correspond to convergence areas ($k_h<0$), whereas lineaments of the second group relate to deceleration areas ($k_v<0$). These lineaments largely indicate strike–slip and dip–slip faults, respectively (Florinsky, 1996). Clearly, an intersection of two lineaments or faults of different groups is associated with a topographically expressed accumulation zone, by its definition (see above). In a

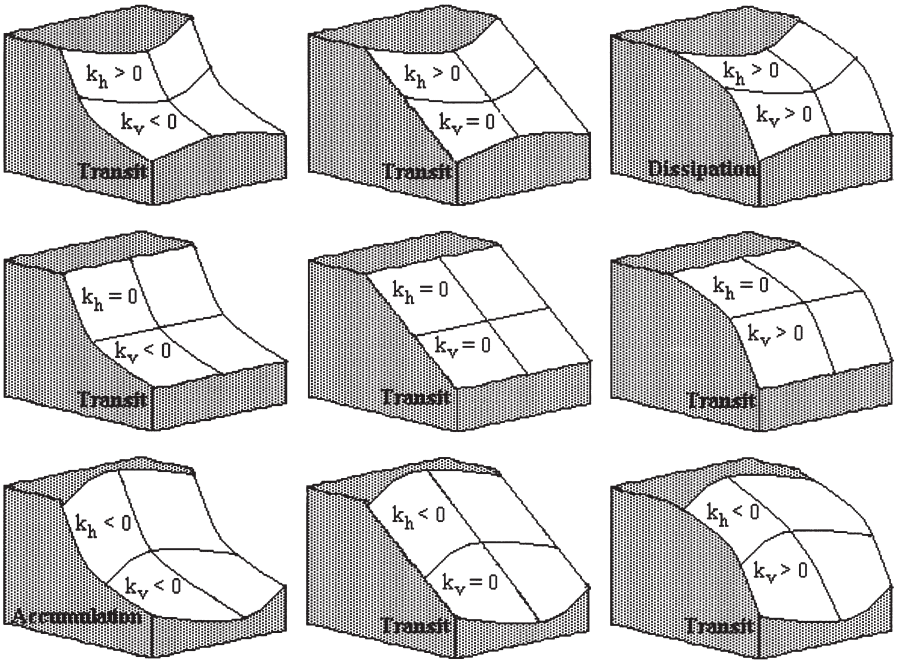


Fig. 1. Classification of landform elements by signs of $k_h$ and $k_v$.

similar manner, a fault segment outside fault intersections and an area between faults relate to transit and dissipation zones, respectively, by their definitions (see above). (We do not maintain that tectonic structures control all accumulation, transit and dissipation zones: certain of them can be formed by pure geomorphic mechanisms.)

The objective of this paper is to investigate comprehensively some interrelationships between fault intersections and topographically expressed accumulation zones, and the function of these sites in landscape evolution. First, we carry out an analysis of associations of sites of fault intersections, intensive rock fracturing and abnormally high discharges of springs and boreholes, relating to fault intersections, with topographically expressed accumulation, transit and dissipation zones. Second, we study the effect of topography on irrigation-induced changes in the salt regime of soils and the groundwater level, assuming that topographically expressed accumulation zones can be marked by the properties of fault intersections.

## 2. Study area

The study area is a part of the Crimean Peninsula measuring about 210 km by 130 km [Figs 2 and 3(a)]. Tectonic elements distinguished within the territory are the Mountain Crimean Alpine meganticlinorium, the Indol–Kuban foredeep and a part of the Scythian Epipalaeozoic plate (Muratov, 1969) [Fig. 3(b)]. Anticlinoria comprise late Triassic and middle Jurassic schists, sandstones and

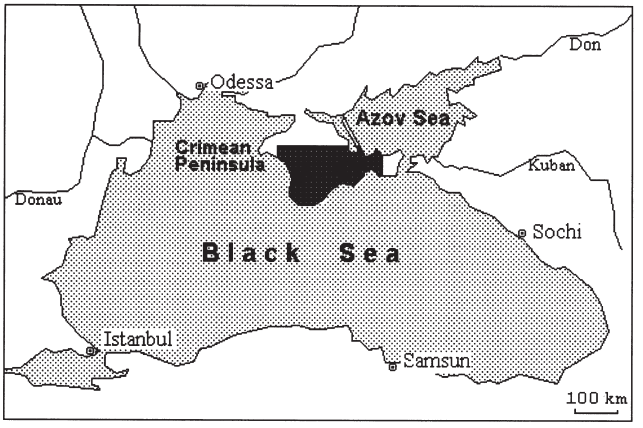


Fig. 2. Geographical location of the study area.

terrigenous flyschs. Synclinoria are formed by late Jurassic and early Cretaceous limestones, sandstones, conglomerates, flyschs and clays. Limbs comprise late Cretaceous, Eocene and Neogene limestones, clays and marls. A pericline is mainly formed by Oligocene–Miocene marine clays. A foredeep predominantly comprises an Oligocene–Quaternary complex. The sedimentary cover of the Scythian plate consists of early and middle Jurassic argillites, aleurolites and conglomerates, late Cretaceous, Paleocene and Eocene clays and carbonate rocks, early Cretaceous, Oligocene, Miocene and Pliocene limestones, clays, marls and sandstones (Muratov, 1969).

Many faults are reflected in the relief of the Crimea (Rastsvetaev, 1977; Sollogub and Sollogub, 1977; Sidorenko, 1980; Kats et al., 1981; Borisenko, 1986; Zaritsky,

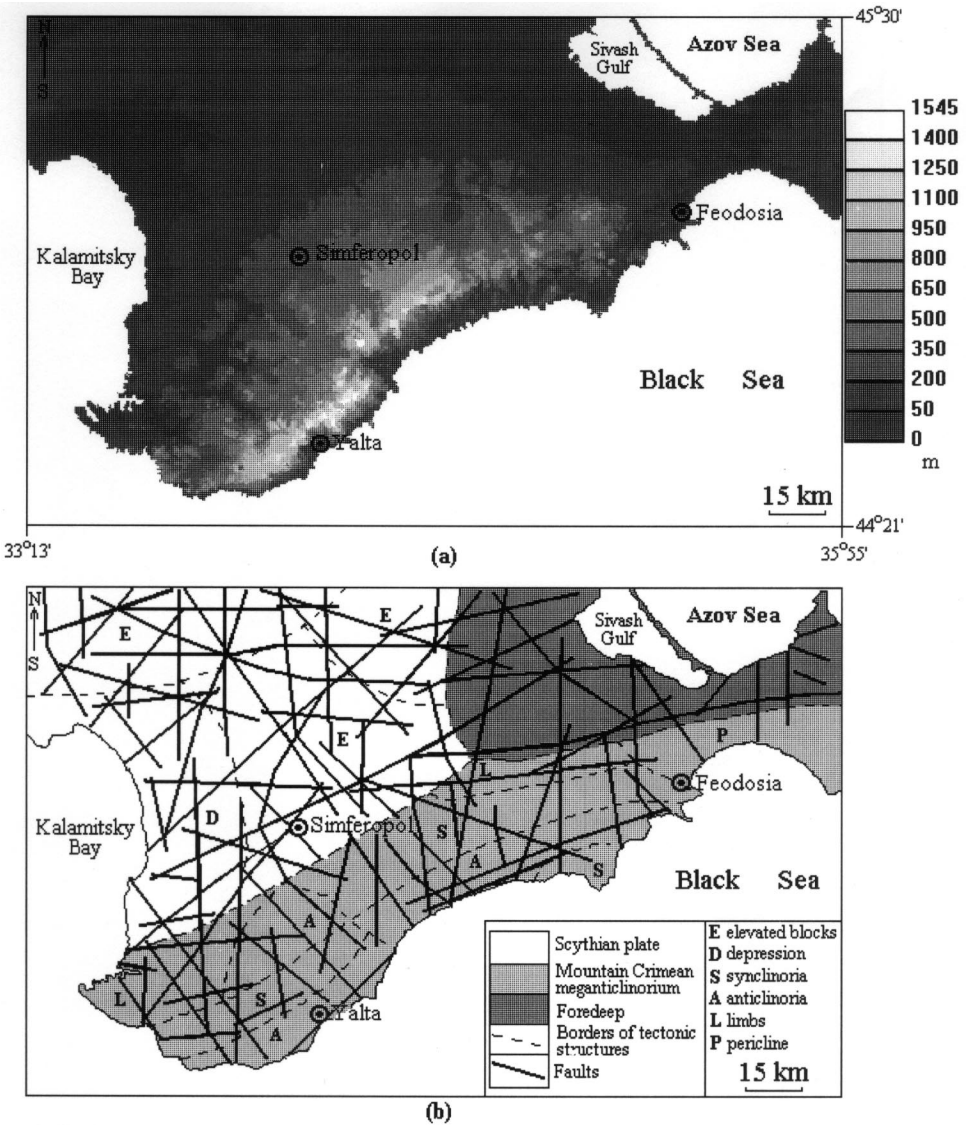


Fig. 3. Part of the Crimean Peninsula: (a) elevation; (b) generalised tectonic scheme.

1989) [Fig. 3(b)]. The study area includes some phenomena relating to fault intersections. For example, sites of increased rock fracturing (Fig. 4) correlate with active faults (Shtengelov 1978, 1982). Sites of abnormally high discharges of springs and boreholes (Fig. 4) as well as discharges of deep-seated thermal groundwaters are found within areas of rock fracturing and at fault intersections (Tkachuk, 1970; Korobeynik et al., 1982; Morozov et al., 1988).

The soil cover of the Plain Crimea largely consists of carbonate Chernozems, Chestnut and Meadow soils, Solonetzs and Solonchaks. Loess-like loam is the dominant parent material (Dzens-Litovskaya, 1970). Chloride–sulphate, chloride and bicarbonate salinisation of soils has been observed (Novikova, 1975) [Fig. 5(a)]. Most of the Plain Crimea is marked by low and medium degrees of salinisation. The most salt-affected areas are flanking the Sivash Gulf, Kalamitsky Bay and the Azov Sea [Fig. 5(a)]. The Plain Crimea is generally medium-drained territory (Novikova, 1975) [Fig. 5(b)]. Small well-drained areas are situated near the Crimean Piedmont. There are poor-drained areas in the northwest and the northeast. Large areas without outflow flank the Sivash Gulf, Kalamitsky Bay and the Azov Sea [Fig. 5(b)].

Since 1963, the Plain Crimea has been irrigated by water of the Dnieper River which is supplied by the North Crimean Canal (NCC) (Minvodkhoz, 1968) [Fig. 5(a)]. There are two branches of the NCC within the study area. The Main branch stretches from the north to the east, while the Krasnogwardeysky branch is located in the northwest. Annual water losses of the NCC range from 25 to 70% of the total water supplied (Lvova, 1982). This has two main causes: (1) waterproof membranes of the Main branch are of a poor quality, and (2) karstified limestones lie below the Krasnogwardeysky branch (Lvova, 1982). Water leaking out of the NCC

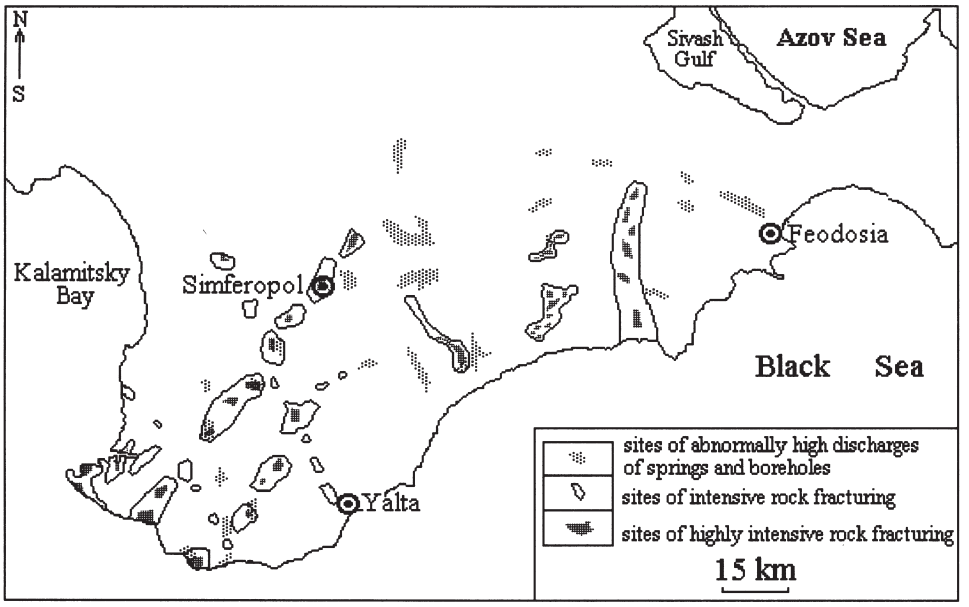


Fig. 4. Phenomena relating to fault intersections within the Crimean Peninsula.

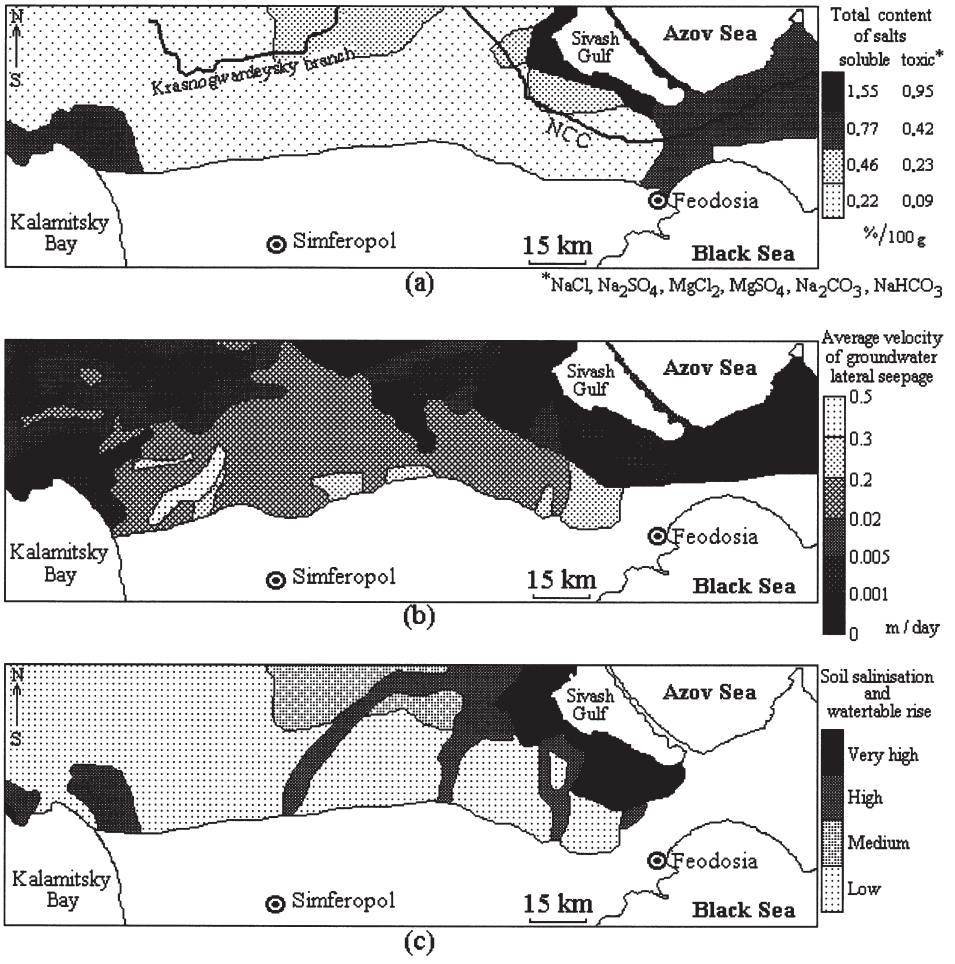


Fig. 5. Salt and groundwater situations within the northern part of the study area: (a) soil salinisation in the aeration zone; (b) natural lateral drainage; (c) forecast regionalisation of irrigation-induced soil salinisation and watertable rise.

causes an increase in soil salinisation due to lateral and vertical redistribution of existing salts (secondary salinisation of soils), as well as a rise of the watertable [Fig. 5(c)] (Novikova, 1975).

Within the Crimean Plain rivers of the northern slope of the Crimean Mountains have poor, irregular overland runoff (mostly in spring), and intensive regular subsurface runoff (Dzens-Litovskaya, 1970). The Main branch of the NCC crosses valleys of these rivers and so plays the role of a geochemical barrier to these natural flows. This also can lead to changes in the salt regime of soils and the groundwater level in adjacent areas.

## 3. Materials and methods

### *3.1. Recognition and mapping of accumulation, transit and dissipation zones*

Recognition of topographically expressed accumulation, transit and dissipation zones can be realised by simple registration of $k_h$ and $k_v$ maps (e.g., Lanyon and Hall, 1983). However, in this case one can visualise only the spatial distribution of these zones without quantitative estimation of a probable degree of flow accumulation. To solve this problem Shary (1995) proposed use of data on the total accumulation ($K_a$) and the mean ($H$) landsurface curvatures:

$$K_a = k_h k_v \tag{1}$$

and

$$H = \frac{1}{2}(k_h + k_v). \tag{2}$$

$K_a$ can be interpreted as a measure of the probable degree of flow accumulation, while $H$ represents flow convergence and acceleration with equal weights. Negative values of $K_a$ correspond to transit zones, while positive values of $K_a$ correspond to both accumulation and dissipation zones. Accumulation and dissipation zones can be distinguished using values of $H$. Positive values of $K_a$ with negative values of $H$ correspond to accumulation zones, whereas positive values of $K_a$ with positive values of $H$ correspond to dissipation zones (Shary, 1995). Recall that fault intersections can be associated with accumulation zones, fault segments outside fault intersections can relate to transit zones, and areas between faults can relate to dissipation zones (Section 1). So, positive values of $K_a$ with negative values of $H$ can relate to fault intersections (Florinsky, 1993), while positive values of $K_a$ with positive values of $H$ can show areas between faults. Negative values of $K_a$ can mark fault segments outside fault intersections.

As the formulae [Eqs. (1) and (2)) suggest, to determine values of $K_a$ and $H$ one should estimate $k_h$ and $k_v$. Once elevations are given by $z=f(x, y)$, where $x$ and $y$ are plane Cartesian coordinates, $k_h$ and $k_v$ are functions of the partial derivatives of $z$ (Shary, 1991):

$$k_h = -\frac{q^2 r - 2pqs + p^2 t}{(p^2+q^2)\sqrt{1+p^2+q^2}} \tag{3}$$

and

$$k_v = -\frac{p^2 r + 2pqs + q^2 t}{(p^2+q^2)\sqrt{(1+p^2+q^2)^3}}, \tag{4}$$

where

$$r = \frac{\delta^2 z}{\delta x^2},\ t = \frac{\delta^2 z}{\delta y^2},\ s = \frac{\delta^2 z}{\delta x \delta y},\ p = \frac{\delta z}{\delta x} \text{ and } q = \frac{\delta z}{\delta y}. \tag{5}$$

Using a square-spaced digital elevation model (DEM), values of $r$, $t$, $s$, $p$ and $q$ can be estimated, for example, by the method of Evans (1979, 1980). In this method, the polynomial

$$z = \frac{rx^2}{2} + \frac{ty^2}{2} + sxy + px + qy + u \tag{6}$$

is approximated by the least-squares method to the 3×3 square-spaced altitude submatrix with a grid mesh of $w$. Points of the submatrix $(-w, w, z_1)$, $(0, w, z_2)$, $(w, w, z_3)$, $(-w, 0, z_4)$, $(0, 0, z_5)$, $(w, 0, z_6)$, $(-w, -w, z_7)$, $(0, -w, z_8)$ and $(w, -w, z_9)$ are measured coordinates and elevations of the landsurface. As a result, we can estimate values of $r$, $t$, $s$, $p$ and $q$ at the point $(0, 0, z_5)$ by the following formulae:

$$r = \frac{z_1 + z_3 + z_4 + z_6 + z_7 + z_9 - 2(z_2 + z_5 + z_8)}{3w^2}, \tag{7}$$

$$t = \frac{z_1 + z_2 + z_3 + z_7 + z_8 + z_9 - 2(z_4 + z_5 + z_6)}{3w^2}, \tag{8}$$

$$s = \frac{z_3 + z_7 - z_1 - z_9}{4w^2}, \tag{9}$$

$$p = \frac{z_3 + z_6 + z_9 - z_1 - z_4 - z_7}{6w} \tag{10}$$

and

$$q = \frac{z_1 + z_2 + z_3 - z_7 - z_8 - z_9}{6w}. \tag{11}$$

Moving the 3×3 submatrix along a DEM, we can calculate values of $r$, $t$, $s$, $p$ and $q$ for all points of the DEM, except boundary points.

We used an irregular DEM of a part of the Crimean Peninsula and the adjacent sea bed as initial data. This DEM was compiled by digitising 1:300,000 and 1:500,000 topographic maps (Central Board of Geodesy and Cartography, 1953; General Headquarters, 1986). The irregular DEM includes 11,936 points. Two regular

DEMs were generated from the irregular one by interpolation using weighted averages (Schut, 1976), we applied grid meshes of 500 m [Fig. 3(a)] and 3000 m. Interpolation and calculations of topographic attributes (see below) were applied both to the dry land and to the sea bed. We do not present results relating to the sea bed since it is not under study.

Digital models of $K_a$ and $H$ were derived from the regular DEM with the grid mesh of 3000 m by the Evans method (see above). A map of topographically expressed accumulation, transit and dissipation zones (Fig. 6) was obtained by combining models of $K_a$ and $H$. These were calculated using a grid spacing of 3000 m for three reasons. First, this reveals landform elements mostly connected with tectonic structure of the study area (Florinsky, 1996). Second, typical sizes of sites of abnormally high discharges of springs and boreholes as well as sites of intensive rock fracturing (Fig. 4) as a whole correspond to typical sizes of accumulation, transit and dissipation zones that can be recognised using this grid mesh (Fig. 6). Third, the grid mesh of 3000 m is best matched to the scale and readability of maps to be obtained (Section 3.3).

### *3.2. Associations of sites of fault intersections, abnormally high discharges of springs and intensive rock fracturing with accumulation, transit and dissipation zones*

We used the following data:

- the map of topographically expressed accumulation, transit and dissipation zones (Fig. 6);
- the map of faults [Fig. 3(b)];
- the map of sites of abnormally high discharges of springs and boreholes (Morozov et al., 1988) (Fig. 4); and
- the map of sites of intensive and highly intensive rock fracturing (Shtengelov 1978, 1980; Korobeynik et al., 1982) (Fig. 4).

The map of faults [Fig. 3(b)] summarises data on main regional faults obtained by geological, geophysical and remote sensing techniques (Muratov, 1969; Rastsvetaev, 1977; Sollogub and Sollogub, 1977; Sidorenko, 1980; Kats et al., 1981; Borisenko, 1986; Zaritsky, 1989).

Sites of abnormally high discharges of springs and boreholes (Fig. 4) correlate with fault intersections (Morozov et al., 1988). These authors did not publish quantitative data on all discharges. An example is the greatest Crimean spring, Karassoo-Bashee, located at one of the fault intersections. Its mean annual discharge is about 1450 l/s (Morozov et al., 1988).

Sites of intensive rock fracturing (Fig. 4) were recognised by a γ-metric method based on a relationship between rock radioactivity and degree of rock fracturing (Shtengelov, 1978). For lithologically homogeneous rocks the greater the rock fracturing, the less γ-activity. This is caused by increased erosive leakage of fine matter that is the major contributor to γ-activity, for most rocks. Shtengelov (1978, 1980) and Korobeynik et al. (1982) did not publish quantitative data on γ-activity of background conditions and sites of intensive and highly intensive rock fracturing.

If accumulation, transit and dissipation zones were evenly distributed in a landscape — that is, their total areas $S_a$, $S_t$ and $S_d$, respectively, were equal — one could estimate the degree of association of a phenomenon with

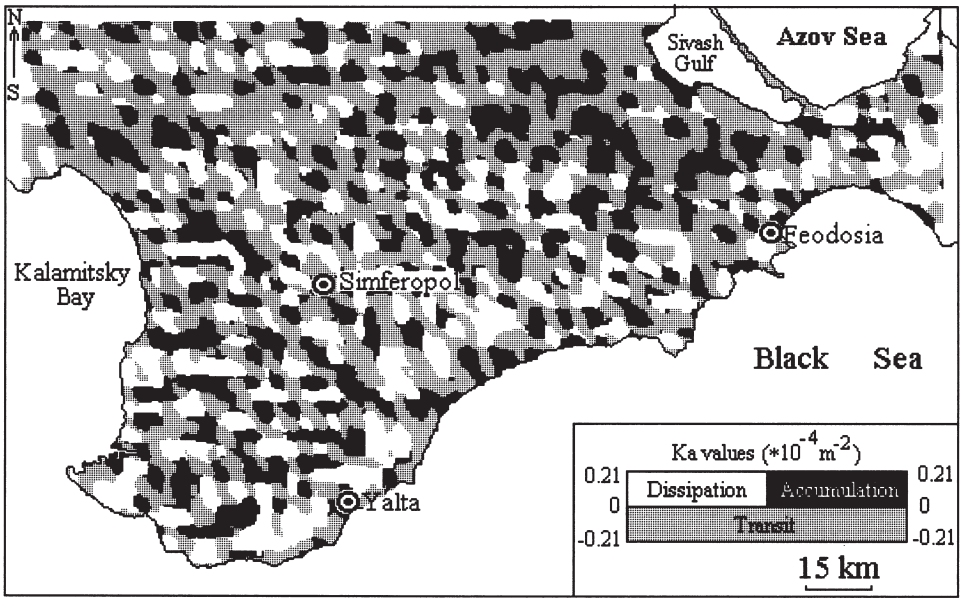


Fig. 6. Topographically expressed accumulation, transit and dissipation zones of the study area.

one or other type of the landsurface zones using a coefficient $P_i=U_i/U_\Sigma$, where $U_i$ is the total area or number of the phenomenon located within each type of landsurface zone and $U_\Sigma$ is the total area or number of the phenomenon. However, from Fig. 6 it is clear that $S_a$, $S_t$ and $S_d$ are not equal. So accumulation, transit and dissipation zones have different 'weights' with relation to associations of interest. Indeed, the apparent association of a phenomenon with one or other type of the landsurface zones can increase with decreasing $S_i$. To estimate the association with regard to differences in $S_i$ one can multiply $P_i$ by 'weights' of accumulation, transit and dissipation zones, $W_a$, $W_t$ and $W_d$, respectively: $W_i=(4/3)-E_i$, where $E_i=S_i/S_\Sigma$ and $S_\Sigma$ is the total area of the study area. If $S_a=S_t=S_d$, so $E_a=E_t=E_d=1/3$ and $W_a=W_t=W_d=1$. If $E_i<1/3$, so $W_i>1$; while if $E_i>1/3$, so $W_i<1$. So, to characterise the association of the phenomenon with one or other type of the landsurface zones, we can use 'an association coefficient', $R_i^{as}=W_iP_i$. $R_i^{as}$ should be normalised; that is, $R_d^{as}+R_t^{as}+R_a^{as}=1$ for each phenomenon.

Hence, we estimated associations of sites of fault intersections, abnormally high discharges and intensive rock fracturing with accumulation, transit and dissipation zones in the following order: (1) determination of $S_a$, $S_t$ and $S_d$ (Table 1); (2) calculation of $E_a$, $E_t$ and $E_d$ (Table 1); (3) evaluation of $W_a$, $W_t$ and $W_d$ (Table 1); (4) estimation of $U_\Sigma$ (Table 2); (5) determination of $U_a$, $U_t$ and $U_d$ (Table 2); (6) calculation of $P_a$, $P_t$ and $P_d$ (Table 2); and (7) estimation of $R_a^{as}$, $R_t^{as}$ and $R_d^{as}$ (Table 2 and Fig. 7).

### *3.3. Effect of topography on irrigation-induced changes in the salt regime of soils and the groundwater level*

We used the following data:

- the map of topographically expressed accumulation, transit and dissipation zones (Fig. 6);
- the map of $k_h$;
- the map of the NCC (Minvodkhoz, 1968) [Fig. 5(a)];
- the map of soil salinisation in the aeration zone (Novikova, 1975) [Fig. 5(a)]; and
- the map of the degree of natural lateral drainage (Novikova, 1975) [Fig. 5(b)].

Table 1
Some parameters of topographically expressed accumulation, transit and dissipation zones within the study area

| Landform element | Parameter | Value |
|---|---|---|
| Accumulation zones | Total area, $S_a$ (km$^2$) | 6588 |
| | Proportion of the total area[a], $E_a$ | 0.25 |
| | Weight, $W_a$ | 1.09 |
| Transit zones | Total area, $S_t$ (km$^2$) | 14,751 |
| | Proportion of the total area[a], $E_t$ | 0.55 |
| | Weight, $W_t$ | 0.78 |
| Dissipation zones | Total area, $S_d$ (km$^2$) | 5364 |
| | Proportion of the total area[a], $E_d$ | 0.20 |
| | Weight, $W_d$ | 1.13 |

[a] The total area of the study area $S_\Sigma=26{,}703$ km$^2$ (without areas relating to boundary columns and rows of the digital models of $K_a$ and $H$).

First, we recognised principal directions of natural flow within the study area. Different approaches can be applied to recognise flow directions by DEM processing (Skidmore, 1990). Since the study is on a broad scale, a crude model of flow directions can be used. $k_h$ maps reflect the spatial distribution of valley networks (e.g., Stepanov, 1989) and hence can be applied to recognise principal directions of natural flow. So, we derived a digital model of $k_h$ from the regular DEM by the method of Evans (1979, 1980) (Section 3.1) with a grid mesh of 3000 m. Then principal directions of natural flow were recognised using the maps of $k_h$ [Fig. 8(a)] and elevation [Fig. 3(a)].

Second, we recognised principal flow directions for water leaking out of the NCC. Maps of the NCC [Fig. 5(a)] and principal directions of natural flow [Fig. 8(a)] were analysed. Principal directions of natural flow located at once downslope from the NCC and intersecting the NCC were assigned to principal directions of probable leakage flow [Fig. 8(a)].

Third, we recognised areas of landscape degradation caused by irrigation, such as secondary salinisation of soils and rise in the watertable. Maps of topographically expressed accumulation, transit and dissipation zones (Fig. 6), the NCC [Fig. 5(a)], principal directions of natural flow and probable leakage flow [Fig. 8(a)] were analysed. To predict these areas we assumed that they relate to accumulation zones (Kovda, 1971). We used the following criterion to recognise an area of probable landscape degradation caused by water leaking out of the NCC [Fig. 8(a)]: an accumulation zone of this sort should be located at once downslope from the NCC and in the path of flows intersecting the NCC. The following condition was applied to recognise an area of probable landscape degradation produced by the NCC as a geochemical barrier [Fig. 8(a)]: an accumulation zone of this type should be situated at once upslope from the NCC and in contact with the NCC and in the path of flows intersecting the NCC.

However, the forecast map of changes in the salt regime of soils and the groundwater level [Fig. 8(a)] represents only the topographic prerequisites of these changes. To adjust this forecast additional non-topographic data have to be used. So, four, we analysed topographic data [Fig. 8(a)] together with data on soil salinisation [Fig. 5(a)] and natural lateral drainage [Fig. 5(b)].

Novikova (1975) argued that territories marked by total soil salinisation below 0.22%/100 g [Fig. 5(a)] can be free of secondary salinisation of soils caused by irri-

Table 2
Parameters of associations of the phenomena under study with topographically expressed accumulation, transit and dissipation zones

| Phenomenon | Total, $U_\Sigma$ | Association parameter | Accumulation zones | Transit zones | Dissipation zones |
|---|---|---|---|---|---|
| Sites of fault intersections | 172 | Total number, $U_i$ | 158 | 9 | 5 |
| | | Proportion of the total number, $P_i$ | 0.92 | 0.05 | 0.03 |
| | | Association coefficient, $R_i^{as}$ | 0.93 | 0.04 | 0.03 |
| Sites of abnormally high discharges of springs and boreholes | 301 km$^2$ | Total area, $U_i$ (km$^2$) | 204 | 90 | 7 |
| | | Proportion of the total area, $P_i$ | 0.68 | 0.30 | 0.02 |
| | | Association coefficient, $R_i^{as}$ | 0.74 | 0.23 | 0.03 |
| Sites of intensive rock fracturing | 1006 km$^2$ | Total area, $U_i$ (km$^2$) | 492 | 382 | 132 |
| | | Proportion of the total area, $P_i$ | 0.49 | 0.38 | 0.13 |
| | | Association coefficient, $R_i^{as}$ | 0.54 | 0.31 | 0.15 |
| Sites of highly intensive rock fracturing | 134 km$^2$ | Total area, $U_i$ (km$^2$) | 95 | 25 | 14 |
| | | Proportion of the total area, $P_i$ | 0.71 | 0.19 | 0.10 |
| | | Association coefficient, $R_i^{as}$ | 0.74 | 0.15 | 0.11 |

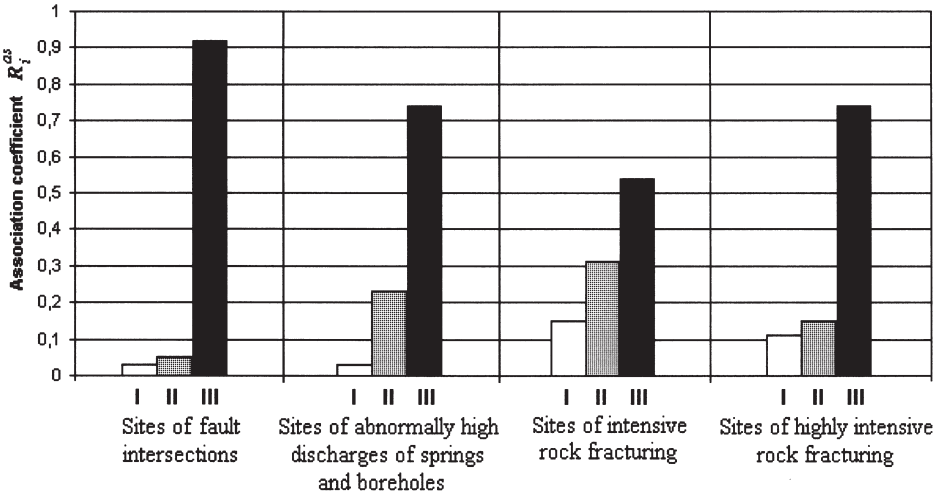


Fig. 7. Association coefficient $R_i^{as}$ of the phenomena under study with topographically expressed dissipation (I), transit (II) and accumulation (III) zones.

gation. Irrigation can result in high, medium and low degrees of secondary soil salinisation within territories marked by the total soil salinisation of 1.55, 0.77 and 0.46%/100 g, respectively [Fig. 5(a)] (Novikova, 1975). However, these changes in salt regime can arise within accumulation zones rather than throughout (Kovda, 1971). So, we ascribed high, medium and low degrees of secondary soil salinisation [Fig. 8(b)] to areas of probable landscape degradation [Fig. 8(a)] within territories marked by the total soil salinisation of 1.55, 0.77 and 0.46%/100 g, respectively [Fig. 5(a)].

Novikova (1975) argued that irrigation can lead to a very high, high, medium, low and very low rise in the watertable within territories marked by a groundwater lateral seepage velocity of below 0.001, 0.001–0.005, 0.005–0.02, 0.02–0.2 and 0.2–0.3 m/day, respectively [Fig. 5(b)]. Territories marked by groundwater lateral seepage velocity above 0.3 m/day [Fig. 5(b)] can be free of irrigation-induced rise in the watertable (Novikova, 1975). However, changes in the groundwater level can arise within topographically expressed accumulation zones rather than throughout. So, we attributed very high, high, medium, low and very low degrees of watertable rise to areas of probable landscape degradation [Fig. 8(a)] within territories marked by groundwater lateral seepage velocities of below 0.001, 0.001–0.005, 0.005–0.02, 0.02–0.2 and 0.2–0.3 m/day, respectively [Fig. 5(b)]. Exceptions are some areas flanking the Krasnogwardeysky branch of the NCC [Fig. 8(a)]. These areas are characterised by groundwater lateral seepage velocity below 0.2 m/day [Fig. 5(b)]. However, there are some limestones with high vertical seepage coefficients, no groundwater in Quarternary deposits, and confined water lying at a depth of 25–100 m there (Novikova, 1975). Therefore, irrigation-induced rise in the watertable cannot arise within these areas. As a result of this study step, we obtained a forecast map of watertable rise [Fig. 8(c)].

We cannot as yet estimate secondary salinisation of

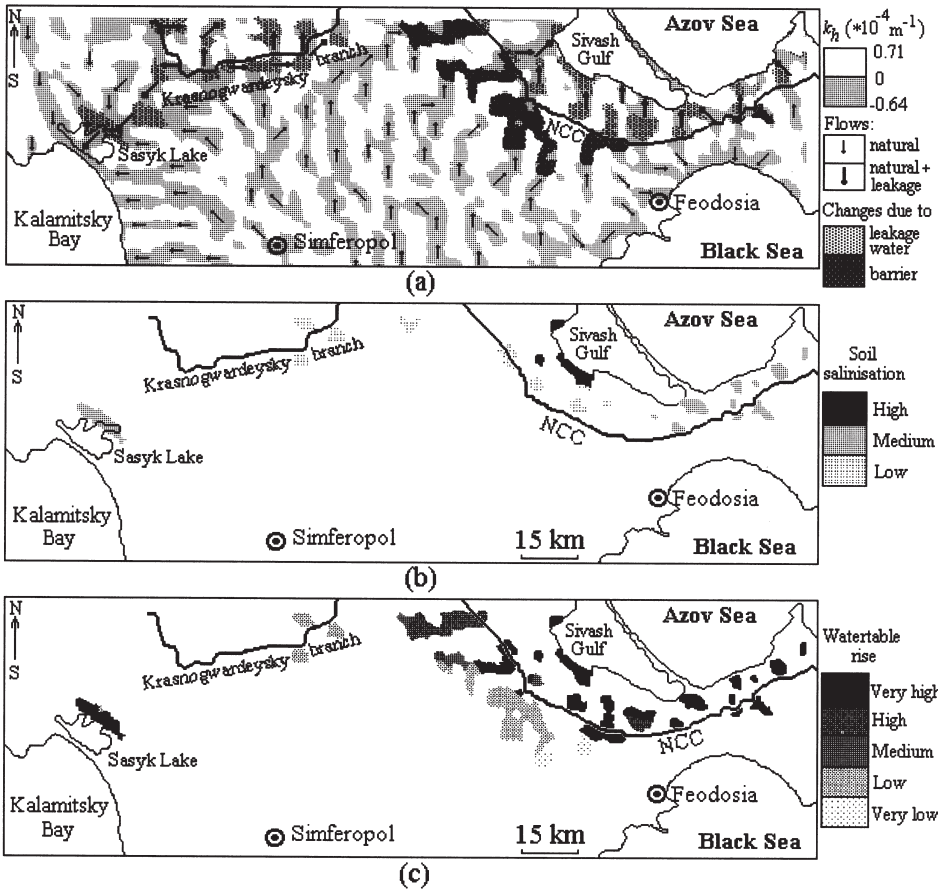


Fig. 8. Forecast maps for the northern part of the study area: (a) irrigation-induced changes in the salt regime of soils and the groundwater level; (b) secondary salinisation of soils; (c) rise in the watertable.

soils and rise in the watertable in absolute units. This may become possible by combining our approach with some established strategies; for example, mathematical modelling of secondary soil salinisation (e.g., Novikova, 1975; Dinar et al., 1993) and water leaking out of canals (e.g., Averyanov, 1982) that are performed without topographic data, and DEM-based hydrological modelling (e.g., Quinn et al., 1991).

Interpolation of the irregular DEM, calculation of $K_a$, $H$ and $k_h$ models, and mapping were performed by the software LANDLORD (Florinsky et al., 1995).

## 4. Results and discussion

### *4.1. Associations of sites of fault intersections, abnormally high discharges of springs and intensive rock fracturing with accumulation, transit and dissipation zones*

The map of topographically expressed accumulation, transit and dissipation zones (Fig. 6) shows an ordered spatial distribution of these landform elements that probably results from intersections of north-, east-, northwest- and northeast-striking regional faults (Florinsky 1992, 1996).

Sites of fault intersections very closely correlate with accumulation zones: the association coefficient is 0.93 (Table 2 and Fig. 7). This is a regular result substantiating facts that accumulation zones often relate to fault intersections (Poletaev, 1992; Florinsky, 1993) (Section 1). Sites of abnormally high discharges and highly intensive rock fracturing closely correlate with accumulation zones: the association coefficients are 0.74 (Table 2 and Fig. 7). This is no surprise: as accumulation zones relate to fault intersections, so phenomena located at fault intersections have to correlate strongly with accumulation zones. Sites of intensive rock fracturing correlate with accumulation zones to a lesser extent: the association coefficient is 0.54 (Table 2 and Fig. 7). At the same time, association between these sites and transit zones is described by the coefficient of 0.31 (Table 2 and Fig. 7). This is also not surprising, since transit zones relate to fault segments outside fault intersections (Section 1). As within these segments fracturing is less than at fault intersections (Fyodorov et al., 1989; Poletaev, 1992), so transit zones can control lesser parts of phenomena typical for accumulation zones. Indeed, associations of sites

of fault intersections, abnormally high discharges and highly intensive rock fracturing with transit zones are described by the coefficients of 0.04, 0.23 and 0.15, respectively (Table 2 and Fig. 7).

The smallest parts of the phenomena under study correlate with dissipation zones: the association coefficient is 0.03 for sites of fault intersections and abnormally high discharges, 0.11 for sites of highly intensive rock fracturing, and 0.15 for sites of intensive rock fracturing (Table 2 and Fig. 7). As dissipation zones or areas between faults are generally devoid of rock fracturing, we anticipate that these results may be artefacts. They can be produced by: (1) some phenomena occurring in accumulation zones of small typical sizes, which would be recognised with a smaller DEM grid mesh than the one used; and (2) data errors. Also, these results can be obtained if some dissipation zones are formed by pure geomorphic processes within sites of fault intersection.

So, a majority of sites of fault intersections, abnormally high discharges of springs and boreholes and intensive rock fracturing coincides with accumulation zones (Table 2 and Fig. 7). Just the same, the results obtained describe trends of association between the phenomena and accumulation zones. These associations can vary with changing geological and geomorphic conditions, study scales and data accuracy: for example, when pure geomorphic mechanisms lead to the formation of accumulation zones on uniform materials or dissipation zones on fractured ones.

Topographically expressed accumulation zones are closely associated with sites of abnormally high discharges and highly intensive rock fracturing (Table 2 and Fig. 7) controlling upward transport of deep-seated groundwater. This result is consistent with an assumption of Lukin (1987) that the most intensive upward recharges of deep-seated confined groundwater from one aquifer to another in accumulation zones are through increased rock fracturing. We suggest that, within accumulation zones, high soil moisture can be controlled by increased upwelling of deep-seated groundwater, coincident with accumulation of overland lateral flows. This statement is consistent with the following established facts:

- increased discharges of springs and boreholes occur both at accumulation zones (Lukin, 1987) and at fault intersections (Morozov et al., 1988);
- increased soil moisture is observed both at accumulation zones (Rode, 1953; Feranec et al., 1991) and at fault intersections (Trifonov et al., 1983);
- increased soil moisture leads to landslide development within accumulation zones (Lanyon and Hall, 1983), as well as at fault intersections (Karakhanyan, 1981); and
- soil development in depressions within fault zones is affected by upwelling of saline and fresh groundwater, together with overland flow carrying dissolved materials. This results in the formation of salt-affected and hydromorphic soils (Kasimov et al., 1978).

The results obtained (Table 2 and Fig. 7) and data cited show that topographically expressed accumulation zones are areas of contact and substance exchange between overland lateral and deep flows. The close association of accumulation zones with sites of abnormally high discharges and highly intensive rock fracturing implies that maps of topographically expressed accumulation, transit and dissipation zones are important in hydrogeology.

### *4.2. Effect of topography on irrigation-induced changes in the salt regime of soils and the groundwater level*

The forecast map of changes in the salt regime of soils and the groundwater level [Fig. 8(a)] demonstrates: (1) principal directions of overland and intrasoil natural flows; (2) principal directions of probable leakage flow; and (3) areas marked by probable accumulation of salts and rise in the watertable. Water leaking out of the NCC can cause secondary salinisation of soils [Fig. 8(b)] and a rise in the watertable [Fig. 8(c)] in some accumulation zones located downslope from the NCC.

Fig. 8(a) shows the predicted migration route of water leaking out of the Krasnogwardeysky branch to Kalamitsky Bay. Lvova (1982) suggested that leakage waters might improve the groundwater condition at the coast, preventing seawater from entering aquifers. However, it is more likely that there will be high secondary salinisation of soils and a rise in the watertable near Sasyk Lake [Fig. 8(b) and (c)]. These processes can lead to a decrease in the quality of brines extracted there and environmental degradation in the region of this health resort.

As a geochemical barrier, the NCC may produce changes in the salt regime of soils and the groundwater level at six areas situated upslope from the NCC [Fig. 8(a)]. However, most of these areas are unimportant in secondary salinisation of soils [Fig. 8(b)]. Instead, this geochemical barrier causes a rise in the watertable within these areas [Fig. 8(c)].

Unfortunately, we cannot perform a rigorous validation of the forecast maps obtained [Fig. 8(b) and (c)]. This is because researchers have not published middle- and small-scaled maps of actual secondary salinisation and watertable rise produced by the NCC operation, although these irrigation effects have been observed in the Crimea (Baer et al., 1974; Novikova, 1975; Alexeev et al., 1989). We can carry out a comparison of the forecast maps obtained [Fig. 8(b) and (c)] with the forecast scheme of irrigation-induced changes in the salt regime of soils and the groundwater level [Fig. 5(c)] (Novikova,

1975). The field studies of Novikova (1975) demonstrated that this regionalisation scheme is rather realistic, but secondary salinisation and rise in the watertable were observed within depressions rather than throughout. Although these depressions were not shown on the Novikova scheme [Fig. 5(c)], they are exactly localised on the forecast maps obtained [Fig. 8(b) and (c)]. This is because we used precise data on the spatial distribution of accumulation zones (Section 3). Qualitative estimation of secondary salinisation of soils and watertable rise within these zones [Fig. 8(b) and (c)] generally correlates with the results of Novikova (1975) [Fig. 5(c)]. So, we suppose that the forecast maps obtained [Fig. 8(b) and (c)] are rather realistic.

Substances concentrated in accumulation zones can be fixed by soils or may be transported over landsurface and in the soil. In addition, substances collected in these zones may be transported through rock fractures, as accumulation zones are associated with intensive rock fracturing (Section 4.1). Therefore, the detrimental effects of the NCC on the landscape can go beyond increased salinisation of soils and rise in the watertable. The decreasing transport of salts can lead to salinisation of the aquifers that are of great importance to the regional economy (Tkachuk, 1970). So, it is worthwhile to monitor groundwater conditions and to implement protective measures in accumulation zones close to canals.

The results obtained (Fig. 8) demonstrate that maps of topographically expressed accumulation, transit and dissipation zones can be used to improve irrigation design, regionalisation and monitoring, as well as for prediction of landscape degradation in territories adjacent to engineering geochemical barriers, such as canals.

## 5. Conclusions

1. Sites of fault intersections, highly intensive rock fracturing and abnormally high discharges, relating to fault intersections, are closely associated with topographically expressed accumulation zones. This demonstrates that, within these zones, the soil moisture is influenced both by upward transport of deep-seated groundwater and by accumulation of overland lateral flows.
2. Water leaking out of the NCC can result in secondary salinisation of soils and a considerable rise in the watertable in some accumulation zones located downslope. As a geochemical barrier, the NCC can produce a high rise in the watertable in some accumulation zones situated upslope. Salts are collected in the accumulation zones, and the slow movement of these substances through rock fractures can lead to the salinisation of aquifers.
3. We believe that accumulation zones are the areas of contact and substance exchange between overland lateral and deep flows.
4. Topographically expressed accumulation zones and fault intersections can be recognised and mapped by DEM processing. Utilisation of these data can be useful to solve some urgent problems of geology, environmental protection, hydrogeology and irrigation.

## Acknowledgements

The author is grateful to Professor E.Ja. Ranzman (Institute of Geography, Russian Academy of Sciences, Moscow), Professor V.G. Trifonov (Geological Institute, Russian Academy of Sciences, Moscow), Dr A.I. Poletaev (Geological Department, Moscow State University) and Dr Yu.I. Fivensky (Geographical Department, Moscow State University) for fruitful discussions, as well as Dr G.L. Andrienko and Dr N.V. Andrienko (Institute of Mathematical Problems of Biology, Russian Academy of Sciences, Pushchino) for the development of some modules of the software LANDLORD. The investigation was performed with partial support from NATO grant Envir. Crg 950218. The author is thankful to Professor F. Bonn and Mr A. Tarussov (Centre d'Aplications et de Recherches en Télédétection, Sherbrooke University, Canada) for instituting this project.

## References

Alexeev, B.A., Alexeeva, N.N., Glazovsky, N.F., Kovaleva, T.A., Kondratyeva, T.I., Kurakova, L.I., Medvedev, A.V., Romanova, E.P., 1989. Ecological Aspects of Irrigation. VINITI, Moscow 224 pp., in Russian.

Averyanov, S.F., 1982. Water Leaking Out of Canals and Its Influence on Groundwater Regime. Kolos, Moscow 237 pp., in Russian.

Baer, R.A., Gogolev, I.N., Lysogorov, S.D., Lyutaev, B.V., Poznyak, S.P., 1974. Some problems of irrigation in conditions of the south of Ukraine. In: Baer, R.A. (Ed.), Irrigation in the USSR. Nauka, Moscow. in Russian

Borisenko, L.S., 1986. Geological criteria of seismic activity in the Crimea. Seismologicheskiye Issledovaniya 9, 38–48 in Russian with English abstract.

Central Board of Geodesy and Cartography, 1953. Topographic Map, scale 1:300,000. Sheets: VI-L-36 (Dzhankoi), VIII-L-36 (Sevastopol), IX-L-36 (Simferopol), V-L-36 (Kherson). Central Board of Geodesy and Cartography of the USSR, Moscow, in Russian.

Dinar, A., Aillery, M.P., Moore, M.R., 1993. A dynamic model of soil salinity and drainage generation in irrigated agriculture: a framework for policy analysis. Water Resources Research 29, 1527–1537.

Dolenko, G.N., Parylyak, A.I., Kopach, I.P., 1967. Conditions of origin and regularities of location for oil-and-gas accumulation areas at the Crimea. In: Dolenko, G.N. (Ed.), Conditions of Origin and Regularities of Location for Oil and Gas Deposits in Ukraine. Naukova Dumka, Kiev. in Russian

Dzens-Litovskaya, N.N., 1970. Soils and Vegetation of the Steppe Crimea. Nauka, Leningrad 157 pp., in Russian.

Evans, I.S., 1979. An integrated system of terrain analysis and slope mapping. Final Report on Grant DA-ERO-591-73-G0040In:, University of Durham, Durham 192 pp.

Evans, I.S., 1980. An integrated system of terrain analysis and slope mapping. Zeitschrift für Geomorphologie (Suppl. Bd.) 36, 274–295.

Fedoseev, A.P., 1959. Soil moisture and terrain topography. In: Konyukhov, N.A. (Ed.), Agricultural Meteorology. Hydrometeorological Press, Moscow. in Russian

Feranec, J., Kolár, J., Krcho, J., 1991. Mapping of the surface water logging intensity of the soils by applying Landsat TM data and complex digital terrain model. Bulletin du Comité Français de Cartographie 127–128, 154–157.

Florinsky, I.V., 1992. Recognition of Lineaments and Ring Structures: Quantitative Topographic Techniques. Pushchino Research Centre Press, Pushchino 47 pp., in Russian with English abstract.

Florinsky, I.V., 1993. Digital elevation model analysis for linear landsurface structure recognition. Abstract of Ph.D. thesis. Moscow State University of Geodesy and Cartography, Moscow 17 pp., in Russian.

Florinsky, I.V., 1996. Quantitative topographic method of fault morphology recognition. Geomorphology 16, 103–119.

Florinsky, I.V., 1998. Combined analysis of digital terrain models and remotely sensed data in landscape investigations. Progress in Physical Geography 22, 33–60.

Florinsky, I.V., Grokhlina, T.I., Mikhailova, N.L., 1995. Landlord 2.0: the software for analysis and mapping of geometrical characteristics of relief. Geodesiya i Cartographiya 5, 46–51 in Russian.

Fyodorov, A.Ye., Azarkin, V.N., Lokshin, B.V., Nogovitsyn, Yu.A., 1989. Methods of Recognition and Investigation of Ore-Bearing Fault Structures. All-Union Scientific Research Institute of Economics of Mineral Raw Material and Prospecting, Moscow 33 pp., in Russian.

Gelfand, I.M., Guberman, Sh.A., Izvekova, M.A., Keilis-Borok, V.I., Ranzman, E.Ja., 1972. Criteria of high seismicity, determined by pattern recognition. Tectonophysics 13, 415–422.

General Headquarters, 1986. Topographic Map, scale 1:500,000. Sheet 12-36-4 (L-36-G), Simferopol. General Headquarters, Moscow, in Russian.

Gerasimov, I.P., Korzhuev, S.S. (Eds.), 1979. Morphostructural Analysis of the Drainage Network of the USSR. Nauka, Moscow 304 pp., in Russian.

Gerrard, A.J., 1981. Soils and Landforms. An Integration of Geomorphology and Pedology. George Allen and Unwin, London 219 pp..

Gurov, V.N., Kertsman, V.M., 1991. Topography as a factor for feasible movement of radionuclides. In: Khitrov, L.M. (Ed.), Geochemical Migration Ways of Artificial Radionuclides in Biosphere, Proceedings of the 5th Conference, Pushchino, December. Vernadsky Institute of Geochemistry and Analytical Chemistry, Moscow, in Russian.

Ivanova, L.S., 1960. The shallow groundwaters in the dry steppes and their relation to the vegetation cover, topography and the soil features. In: Victorov, S.V. (Ed.), Problems of Indicative Geobotany. The Moscow Society of Naturalists, Moscow. in Russian with English abstract

Karakhanyan, A.S., 1981. Recognition of amply-dimensional landslides and rock blocks torn and slipped down by gravity with the use of remotely sensed data. Izvestiya Vysshikh Uchebnykh Zavedeny, Geologiya i Razvedka 3, 130–131 in Russian.

Kasimov, N.S., Kovin, M.I., Proskuryakov, Y.V., Shmelkova, N.A., 1978. Geochemistry of the soils of fault zones (examplified by Kazakhstan). Soviet Soil Science 10, 397–406.

Kats, Ja.G., Makarova, N.V., Kozlov, V.V., Trofimov, D.M., 1981. Geological and geomorphological study of the Crimea by remotely sensed data interpretation. Izvestiya Vysshikh Uchebnykh Zavedeny, Geologiya i Razvedka 3, 8–20 in Russian.

Kerrich, R., 1986. Fluid transport in lineaments. Philosophical Transactions of the Royal Society of London, A. Mathematical and Physical Sciences 317, 219–251.

Kirkby, M.J., Chorley, R.J., 1967. Throughflow, overland flow and erosion. Bulletin of the International Association of Scientific Hydrology 12, 5–21.

Korobeynik, V.M., Komarova, M.V., Shtengelov, Ye.S., 1982. Permeable-faults of the Earth crust in the Crimea and the north-western Black Sea area. Doklady Academii Nauk Ukrainskoi SSR, Series B 2, 13–16 in Russian with English abstract.

Kovda, V.A., 1971. Origin of Saline Soils and Their Regime. vol. 1. Israel Program for Scientific Translations, Jerusalem 509 pp.

Krcho, J., 1983. Theoretical conception and interdisciplinary application of the complex digital model of relief in modelling bidimensional fields. Geografický Časopis 35, 265–291 in Slovak with English abstract.

Kutina, J., 1969. Hydrothermal ore deposits in the western United States: a new concept of structural control of distribution. Science 165, 1113–1119.

Lanyon, L.E., Hall, G.F., 1983. Land surface morphology. Soil Science 136, 382–386.

Lukin, A.A., 1987. Experience in Development of Morphostructural and Hydrological Analysis Technique. Nauka, Novosibirsk 111 pp., in Russian.

Lvova, Ye.V., 1982. Plains of the Crimea. Tavria, Simferopol 80 pp., in Russian.

Meshcheryakov, Yu.A., 1965. Structural Geomorphology of Plain Lands. Nauka, Moscow 390 pp., in Russian.

Minvodkhoz, 1968. Irrigation systems of the North Crimean Canal. In: Irrigation Systems of the USSR, No. 2, Ukrainian Soviet Socialist Republic. Minvodkhoz, Moscow, pp. 7–18. in Russian

Moore, I.D., Grayson, R.B., Ladson, A.R., 1991. Digital terrain modelling: a review of hydrological, geomorphological and biological applications. Hydrological Processes 5, 3–30.

Morozov, V.I., Kovalenko, A.P., Pasynkov, A.A., 1988. Sites of abnormally high discharges of the Crimean Mountains. Geologichesky Zhurnal 2, 65–69 in Russian with English abstract.

Muratov, M.V. (Ed.), 1969. Geology of the USSR, vol. 8, The Crimea, Part 1, Geological Description. Nedra, Moscow 575 pp., in Russian.

Novikova, A.V., 1975. Prediction of Secondary Salinisation of Soils Produced by Irrigation. Estimation of Terrain Suitability for Irrigation Examplified by the South Part of the Ukrainian Soviet Socialist Republic. Urozhai, Kiev 184 pp., in Russian.

Ollier, C., 1981. Tectonics and Landforms. Longman, London 324 pp..

Pennock, D.J., Zebarth, B.J., De Jong, E., 1987. Landform classification and soil distribution in hummocky terrain, Saskatchewan, Canada. Geoderma 40, 297–315.

Poletaev, A.I., 1992. Fault Intersections of the Earth Crust. Geoinformmark, Moscow 50 pp., in Russian.

Quinn, P.F., Beven, K.J., Chevallier, P., Planchon, O., 1991. The prediction of hillslope flowpaths for distributed modelling using digital terrain models. Hydrological Processes 5, 59–80.

Rastsvetaev, L.M., 1977. The Mountain Crimea and the North Black Sea area. In: Suvorov, A.I. (Ed.), Faults and Horizontal Movements of Mountain Chain of the USSR. Nauka, Moscow. in Russian

Rode, A.A., 1953. Toward the origin of microrelief of the Northern Caspian Lowland. In: Glazovskaya, M.A., Gvozdetsky, N.A. (Eds.), Problems of Geography. Geographizdat, Moscow. in Russian

Schut, G.H., 1976. Review of interpolation methods for digital terrain models. The Canadian Surveyor 30, 389–412.

Shary, P.A., 1991. The second derivative topographic method. In: Stepanov, I.N. (Ed.), The Geometry of the Earth Surface Structures. Pushchino Research Centre Press, Pushchino. in Russian

Shary, P.A., 1995. Land surface in gravity points classification by complete system of curvatures. Mathematical Geology 27, 373–390.

Shary, P.A., Kuryakova, G.A., Florinsky, I.V., 1991. On the international experience of topographic methods employment in landscape investigations (a concise review). In: Stepanov, I.N. (Ed.), The Geometry of the Earth Surface Structures. Pushchino Research Centre Press, Pushchino. in Russian

Shtengelov, Ye.S., 1978. On the fan-like recent spreading of the Earth crust and on the nature of Benioff zones. Doklady Academii Nauk SSSR 240, 922–925 in Russian.

Shtengelov, Ye.S., 1980. Effect of well exploitation of the Upper Jurassic aquifer on seismicity of the Crimea. Water Resources 7, 132–139.

Shtengelov, Ye.S., 1982. Zones of recent and modern spreading of continental crust. International Geology Review 24, 759–770.

Sidorenko, A.V. (Ed.), 1980. Map of Faults of the USSR and Territories of Adjacent States, scale 1:2,500,000. Aerogeologiya, Moscow 20 pp., in Russian.

Skidmore, A.K., 1990. Terrain position as mapped from a gridded digital elevation model. International Journal of Geographical Information Systems 4, 33–49.

Sollogub, V.B., Sollogub, N.V., 1977. Structure of the earth crust of the Crimean Peninsula. Sovetskaya Geologiya 3, 85–93 in Russian.

Speight, J.G., 1974. A parametric approach to landform regions. In: Brown, E.H., Waters, R.S. (Eds.), Progress in Geomorphology. Papers in Honour of D.L. Linton. Institute of British Geographers, London.

Stepanov, I.N. (Ed.), 1989. Map of Landsurface Systems and Soil Cover of the Part of the Middle Asia, scale 1:1,500,000. The Central Board of Geodesy and Cartography of the Council of Ministers of the USSR, Moscow 2 pp., in Russian.

Tkachuk, V.G. (Ed.), 1970. Hydrogeology of the USSR, vol. 8. The Crimea. Nedra, Moscow 364 pp., in Russian.

Trifonov, V.G., Makarov, V.I., Safonov, YU.G., Florensky, P.V. (Eds.), 1983. Space Information for Geology. Nauka, Moscow 535 pp., in Russian with English contents.

Troeh, F.R., 1964. Landform parameters correlated to soil drainage. Soil Science Society of America Proceedings 28, 808–812.

Wood, E.F., Sivapalan, M., Beven, K.J., 1990. Similarity and scale in catchment storm response. Reviews of Geophysics 28, 1–18.

Yefremov, Yu.K., 1949. An experience on morphological classification of elements and simple forms of relief. In: Salishchev, K.A., Komkov, A.M. (Eds.), Problems of Geography, No. 11, Cartography. Geographizdat, Moscow. in Russian

Young, A., 1972. Slopes. Oliver and Boyd, Edinburgh 288 pp..

Zaritsky, A.I. (Ed.), 1989. Map of Linear and Ring Structures of the Ukrainian Soviet Socialist Republic (by Remotely Sensed Data), scale 1:1,000,000. Ukrgeologiya, Kiev 4 pp., in Russian.